Noname manuscript No.
(will be inserted by the editor)

Cellular coverage probability is independent of base station density under stochastic geometric model

H. Nassar[1] · **G. Taher** [1] · **S. El-Hady** [2]

the date of receipt and acceptance should be inserted later

Abstract Stochastic geometry (SG) has been extensively used to model cellular communications, under the assumption that the base stations (BS) are deployed as a Poisson point process in the Euclidean plane. This use has spawned a huge number of articles over the past years for different scenarios, culminating in an equally huge number of expressions for the coverage probability in both the uplink (UL) and downink (DL) cellular directions. The problem is that those expressions include the BS density, λ, which we prove irrelevant in this article. We start by developing a SG model for a baseline cellular scenario, then prove that its coverage probability is independent of λ, contrary to popular belief.

Keywords Stochastic geometry; Cellular network; Base station density; Coverage probability; Downlink; Uplink

1 Introduction

Stochastic geometry (SG) has been used heavily in the last decade as a modelling tool for wireless communications. It treats the network as a realization (snapshot) of a spatial point process in the Euclidean plane [Haenggi, 2012]. In this respect, it provides a natural approach to describe node locations in randomly formed networks, e.g. ad hoc and cellular networks.

The most common task of SG in wireless communications is to characterize the signal to interference and noise ratio (SINR), which can then be used to calculate many cellular performance metrics, such as outage probability, coverage probability,

Hamed Nassar
E-mail: nassar@ci.suez.edu.eg
Gehad Taher
E-mail: gehad.taher@ci.suez.edu.eg
S. El-Hady
E-mail: elsayed_elhady@ci.suez.edu.eg
[1]Computer Science Department, Faculty of Computers and Informatics Suez Canal University, Ismailia, Egypt.

spatial opportunity, spatial throughput, network throughput, medium access probability and spectral efficiency [Okegbile et al., 2021], in both the downlink (DL) and uplink (UL) directions. It should be noted, however, that in light of the huge influx of wireless emissions in recent years, the impact of noise now pales in comparison with interference [Liu et al., 2020b]. As such, there is a growing trend (see, for example, [Tang et al., 2020, Liu and Zhang, 2020, Haroon et al., 2021, Kouzayha et al., 2021]) to replace SINR by SIR, and we will follow this trend in the present article.

The assumption that is often made when SG is used in modelling cellular networks is that base stations (BS) are deployed in the Euclidean plane as a Poisson Point Process (PPP) [ElSawy et al., 2017]. However, other variant processes, e.g. Thomas cluster processes or Matérn cluster processes, have been used as well [Blaszczyszyn et al., 2018].

The SG model replaces the once popular hexagonal grid model, in which base stations were placed at the centers of the hexagonal lattices. It has been shown [Lee et al., 2013] that the PPP approach provides much more accurate results than the hexagonal grid model when both are used to model real world cellular installation. It has also been shown [Andrews et al., 2011] that the PPP model gives lower bounds, whereas the hexagonal model gives upper bounds, of the coverage probability, which means that the former is safer to rely on.

SG cellular models that end up with coverage probability expressions involving the BS density, λ, abound. Examples of such models for DL are [ElSawy et al., 2017, Liu et al., 2020b, Liu and Zhang, 2020, Kouzayha et al., 2021, Bai and Heath, 2015, Chen and Yuan, 2019, Liu et al., 2020a, Ouamri et al., 2020, Lei et al., 2018, Fadouol, 2020, Gao et al., 2019, Ali et al., 2019, Andrews et al., 2016, Kundu et al., 2020, Sadeghabadi et al., 2020, Wang and Gursoy, 2019]. On the other hand, examples of such models for DL are [ElSawy et al., 2017, Liu et al., 2020b, Haroon et al., 2021, Herath et al., 2018, Kouzayha et al., 2018, Mariam et al., 2021, Andrews et al., 2016, Jia et al., 2019, Gao et al., 2019, Ali et al., 2019, Kundu et al., 2020, Sadeghabadi et al., 2020, Wang and Gursoy, 2019]. We will shortly prove that under the SG model, the cellular coverage probability is independent of λ, both in DL and UL.

To set the stage for these theorems, we will first develop a SG model for a baseline scenario. Next, we will use the model to derive two expressions for the coverage probability, in DL and UL, which will include λ, just like the above cited models. Then we will manipulate these expressions to prove that λ is superfluous.

It is worth mentioning that the notion that the coverage probability is independent of λ has only been alluded to sparingly previously. The authors of [Bai and Heath, 2015], in the context of analyzing DL coverage probability of millimeter-wave cellular networks, noted that "coverage does not scale with BS density." Also, the authors of [Herath et al., 2018], while analyzing UL FPC, noted that coverage is " invariant to the density of deployment of BSs when the shadowing is mild and power control is fractional." To the best of our knowledge, the present article is the first to provide a rigorous proof that the coverage probability is independent of the BS density.

The rest of the article is organized as follows. In Section 2, we develop SG models for DL and UL, and use these models to prove that the coverage probability is independent of the BS density λ. Section 3 has the conclusions.

2 System Model

We consider a cellular network made up of a BS, each serving a number of user equipments (UEs). The main assumption we make is that the BSs are located according to a 2D PPP Φ, of intensity λ in the Euclidean plane.

which effectively means they are randomly scattered in the Euclidean plane with independent locations [Blaszczyszyn et al., 2018]. We consider orthogonal communications within each cell, meaning that in each cell there can be only one active UE on any time/frequency resource. Accordingly, Figure 1 is a snapshot of the UEs that are active on the same frequency in all the cells at the same time. As for the entire network, every BS-UE pair shown in the Figure is operating on the same resource, hence is the interference that we are going to characterize.

Some definitions used throughout the article are now in order.

Definition 1 (BS-UE association): BS-UE association is the assignment of a UE to a BS, for both to establish a communications session.

Definition 2 (Serving BS): Once a UE is associated with a BS, the latter is said to be the serving BS of the UE.

Definition 3 (Typical receiver): The typical receiver is the receiving device (UE or BS) where the SIR is to be assessed. It is always placed at the origin of the Euclidean plane in the model, or the origin of the simulation window in the simulation.

Definition 4 (Tagged transmitter): The tagged transmitter is transmitting device (UE or BS) associated with the typical receiver.

Definition 5 (Typical circle): The typical circle is the circle centered at the typical receiver and having the tagged transmitter on its circumference.

Definition 8 (Interferer): An interferer is a transmitter causing interference at the typical receiver. That is, it is any transmitter in the network other than the tagged transmitter.

Definition 9 (Signal to Interference Ratio (SIR)): The quotient of the signal at the typical receiver and the sum of all interferences at the typical receiver.

As per Definitions 3 and 4, in DL the typical receiver is a UE and the tagged transmitter is a BS, whereas in UL the typical receiver is a BS and the tagged transmitter is a UE.

A UE will associate with the BS nearest it. We will denote the distance between the two elements of a BS-UE pair throughout by R. It can then be shown that R is a random variable (RV) with the Rayleigh distribution

$$f_R(r) = 2\lambda\pi r e^{-\lambda\pi r^2}, \qquad r \geq 0 \tag{1}$$

The notation used throughout the article is provided in Table 1.

Table 1: Notation used in the model.

Parameter	Description
BS	Base station
UE	User Equipment (can be a mobile phone, tablet, laptop, etc.)
Φ	Poisson point process (PPP) of BSs
Ψ	Point process of UEs (not Poisson)
λ	Density of BS (per m^2), i.e. intensity of PPP Φ
α	Path-loss exponent (per m)
SIR	Signal to interference ratio (dB)
ξ	SIR threshold (dB)
G	Rayleigh channel gain of tagged transmitter ($G \sim Exp(1)$)
p	Transmit power (Watts)
p_d	DL coverage probability
p_u	UL coverage probability

Referring to Figure 1, the typical receiver resides at the origin, and the tagged transmitter resides on the perimeter of the typical circle. In part 1a, we see the DL model, where the typical receiver is a UE, and the tagged transmitter is a BS at distance R. All the BSs outside the typical circle are interferers to the typical UE. In part 1b, we can see the UL model, where the typical receiver is a BS, and the tagged transmitter is a UE at distance R. All the UEs except the tagged are interferers to the typical BS.

Random channel effects are incorporated by multiplicative RVs, namely G for the signal and G_i for each interferer i. For simplicity we assume small-scale Rayleigh fading, and assume G and the G_i iid RVs following an exponential distribution with mean 1. In addition, we assume that signals attenuate with distance according to the standard power-law path loss propagation model, with path loss exponent $\alpha > 2$. That is, the average received power at distance r from a transmitter of power p is $pr^{-\alpha}$ [Blaszczyszyn et al., 2018].

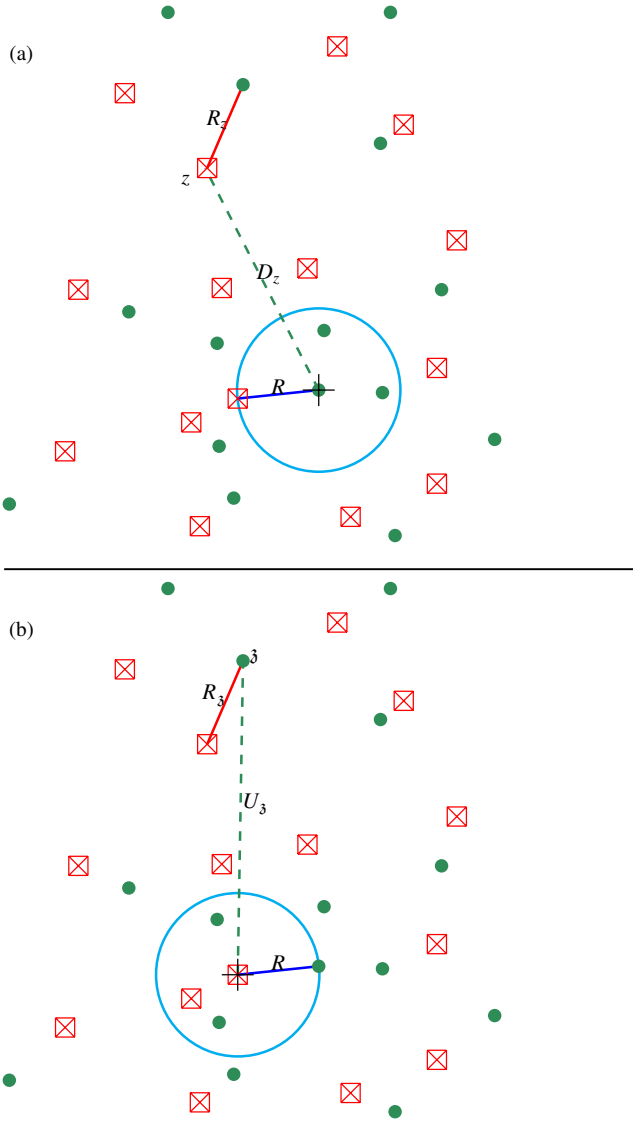

Fig. 1: Two stochastic geometric models for assessing the SIR at a typical receiver in the same cellular network. (a) The DL model, where the typical receiver is a UE. The typical circle defines an exclusion zone, as it cannot contain a BS inside. The BSs outside the typical circle, which cause interference at the typical UE, form a PPP Φ. (b) The UL model, where the typical receiver is a BS. The typical circle does not define an exclusion zone, as it can contain UEs inside. The UEs inside and outside the typical circle form a PP Ψ. Since the UEs are *s*atellites to their serving BSs, as per the association rule, Ψ is not Poisson—a major challenge. We mitigate this challenge by relocating each UE, except the tagged, to the position of its serving BS.

2.1 Downlink model

The key assumptions of the DL system model are:

- A UE wishing to start a communications session associates with the BS that is closer to it than any other BS in the cellular network (association rule.)
- The BS transmits at a fixed power p to the associated UE on a particular time-frequency resource, i.e. orthogonal communications within the cell. The consequence of orthogonality is that the UE sees interference from all the BSs in the plane, except its serving BS.
- Random channel effects are incorporated by a multiplicative RVs G for the signal and G_z for every interferer at z. For simplicity we assume these correspond to Rayleigh fading with mean 1, so G and the G_z are iid RVs, having exponential distribution with mean 1.

Let I_d denote the interference experienced at the typical UE. The interference is due to every BS z in the plane, except the tagged BS, denoted by $\mathfrak{b}$, at distance D_z from the typical UE, as shown in Figure 1a. That is, the interference I_d is created by a PPP with intensity λ outside the typical circle, and is given by

$$I_d = \sum_{z \in \Phi \setminus \{\mathfrak{b}\}} p G_z D_z^{-\alpha}, \tag{2}$$

where p is the power of the BS at point z, and D_z is a RV representing the distance from the BS at za and the typical UE. The SIR at the typical UE is then given by

$$\mathtt{SIR}_{\mathrm{UE}} = \frac{pGR^{-\alpha}}{I_d} \tag{3}$$

The goal now is to derive the DL coverage probability p_d, which is exactly the complementary cumulative distribution function (CCDF) of SIR over the entire network (Recall that the CDF gives $\mathbb{P}[\mathrm{SIR} \leq \xi]$). The coverage probability can also be visualized as the probability that a randomly chosen user can achieve a target SIR ξ, the average fraction of users who at any time achieve SIR ξ, or the average fraction of network area that is in "coverage" at any time.

We start by invoking the concept of total probability, using (2) and (3), to get

$$\begin{aligned}
p_{d|R} &= \mathbb{P}[\mathtt{SIR}_{\mathrm{UE}} > \xi] \\
&= \mathbb{P}\left[\frac{pGR^{-\alpha}}{I_d} > \xi\right] \\
&= \mathbb{P}\left[G > \frac{\xi}{p} R^{\alpha} I_d\right] \\
&\overset{(a)}{=} \mathbb{E}_{I_d}\left[\mathbb{P}\left[G > \frac{\xi}{p} R^{\alpha} I_d\right]\right] \\
&\overset{(b)}{=} \mathbb{E}_{I_d}\left[e^{-\frac{\xi}{p} R^{\alpha} I_d}\right] \\
&\overset{(c)}{=} \mathscr{L}_{I_d}\left(\frac{\xi}{p} R^{\alpha}\right)
\end{aligned} \tag{4}$$

where

$$\mathscr{L}_A(s) = \int_0^\infty e^{-st} f_A(t)dt = \mathbb{E}\left[e^{-sA}\right] \tag{5}$$

is the Laplace transform of the RV I_d conditioned on the RV R between the typical UE and the tagged BS. In (a) we utilized the fact that we can write a probability $\mathbb{P}[A > B)]$ as $\mathbb{E}_B[\mathbb{P}[A > B]]$ (or $\mathbb{E}_A[\mathbb{P}[A > B]]$), in (b) we benefited from the fact that $G \sim \exp(1)$, i.e. $f_G(r) = e^{-r}$, and in (c) we used the Laplace transform definition (5).

Clearly, the DL coverage probability p_d in (4) is conditioned on R, the distance between the typical UE and the tagged BS. We will now embark on deconditioning p_d. Since R is the distance between the typical UE and the closest BS (the tagged BS), it is Rayleigh distributed, i.e. and $f_R(r) = 2\lambda\pi re^{-\lambda\pi r^2}$ from (1). Further, R ranges from an arbitrarily small positive real number greater than 0 (to exclude the typical UE) to ∞. Thus, the conditional coverage probability

$$\begin{aligned} p_{d|R} &= \mathbb{E}_R\left[p_{d|R}\right] \\ &= \mathbb{E}_R\left[\mathscr{L}_{I_d}(\frac{\xi}{p}R^\alpha)\right] \\ &= \int_0^\infty \mathscr{L}_{I_d}(\frac{\xi}{p}r^\alpha) f_R(r)dr \\ &= 2\lambda\pi\int_0^\infty e^{-\lambda\pi r^2}\mathscr{L}_{I_d}(\frac{\xi}{p}r^\alpha)rdr \end{aligned} \tag{6}$$

Next, we will embark on finding the Laplace transform $\mathscr{L}_{I_d}$ of the DL interference I_d. Using (2) and (5), we get

$$\begin{aligned} \mathscr{L}_{I_d}(s) &= \mathbb{E}\left[e^{-sI_d}\right] \\ &= \mathbb{E}_{\Phi,G_z}\left[e^{-s\sum_{z\in\Phi\setminus\{\mathfrak{b}\}} pG_zD_z^{-\alpha}}\right] \\ &= \mathbb{E}_{\Phi,G_z}\left[\prod_{z\in\Phi\setminus\{\mathfrak{b}\}} e^{-spG_zD_z^{-\alpha}}\right] \\ &\overset{(a)}{=} \mathbb{E}_\Phi\left[\prod_{z\in\Phi\setminus\{\mathfrak{b}\}} \mathbb{E}_{G_z}\left[e^{-spG_zD_z^{-\alpha}}\right]\right] \\ &\overset{(b)}{=} \mathbb{E}_\Phi\left[\prod_{z\in\Phi\setminus\{\mathfrak{b}\}} \mathscr{L}_{G_z}(spD_z^{-\alpha})\right] \\ &\overset{(c)}{=} \exp\left(-\lambda\int_{\mathbb{R}^2\setminus D(o,r)}(1-\mathscr{L}_{G_z}(spD_z^{-\alpha}))\right) \end{aligned} \tag{7}$$

where $D(o,r)$ is a disc centered at the origin and has a radius r. In (a) we benefited from the independence of the G_z, which are iid and in (b) we used the definition (5) of the Laplace transform. In (c), to decondition on D_z which is distributed *differently* for each point z of the PPP, we invoked the PGFL $\mathbb{E}_\Phi\left[\prod_{z\in\Phi} f(x)\right]$, with

$f(x) = \mathscr{L}_{G_z}(spx^{-\alpha})$, of the PPP Φ. Switching to polar coordinates, with the interferer now at $(x,\theta) \in \mathbb{R}^2$, then using the fact that $G_z \sim \exp(1)$, i.e. $f_{G_z}(t) = e^{-t}$, then Using (7) yields

$$\begin{aligned}\mathscr{L}_{I_d}(s) &= \exp\left(-\lambda \int_0^{2\pi}\int_r^{\infty}(1-\mathscr{L}_{G_z}(spx^{-\alpha}))xdxd\theta\right)\\ &= \exp\left(-2\pi\lambda\int_r^{\infty}(\frac{spx^{-\alpha}}{1+spx^{-\alpha}})xdx\right)\end{aligned} \tag{8}$$

For use in (6), we write this result as

$$\begin{aligned}\mathscr{L}_{I_d}(\frac{\xi}{p}r^{\alpha}) &= \exp\left(-2\pi\lambda\int_r^{\infty}(\frac{(\frac{\xi}{p}r^{\alpha})px^{-\alpha}}{1+(\frac{\xi}{p}r^{\alpha})px^{-\alpha}})xdx\right)\\ &= \exp\left(-\pi\lambda r^2\xi^{\frac{2}{\alpha}}\int_{\xi^{-2/\alpha}}^{\infty}\frac{1}{1+u^{\alpha/2}}du\right)\end{aligned}$$

where $u = (x/r)^2\,\xi^{-\frac{2}{\alpha}}$. Substituting this in (6), we get

$$p_d = 2\widetilde{\lambda}\int_0^{\infty} e^{-\widetilde{\lambda}r^2} e^{-\widetilde{\lambda}r^2\sqrt[\kappa]{\xi}\int_{\frac{1}{\sqrt[\kappa]{\xi}}}^{\infty}\frac{1}{1+u^{\kappa}}du} rdr \tag{9}$$

where $\widetilde{\lambda} = \lambda\pi$ and $\kappa = \alpha/2$.

From (9), it *appears* that the DL coverage probability p_d is dependent on the BS density λ. However, this dependence is false, as we will show in the next Theorem.

Theorem 1: Under the stochastic geometric model of the cellular DL system, the DL coverage probability p_d is independent of the BS density λ.

Proof: The proof is attained through two changes of variables. Starting with (9), use the substitution $x = r^2$ to get

$$\begin{aligned}p_d &= 2\widetilde{\lambda}\int_0^{\infty} e^{-\widetilde{\lambda}r^2} e^{-\widetilde{\lambda}r^2\xi^{\frac{2}{\alpha}}\int_{\xi^{-\frac{2}{\alpha}}}^{\infty}\frac{1}{1+u^{\kappa}}du} rdr\\ &= \widetilde{\lambda}\int_0^{\infty} e^{-\widetilde{\lambda}x\left(1+\sqrt[\kappa]{\xi}\int_{\frac{1}{\sqrt[\kappa]{\xi}}}^{\infty}\frac{1}{1+u^{\kappa}}du\right)}dx\end{aligned}$$

Now use the substitution $z = \widetilde{\lambda}x$ to get

$$\begin{aligned}p_d &= \int_0^{\infty} e^{-z\left(1+\sqrt[\kappa]{\xi}\int_{\frac{1}{\sqrt[\kappa]{\xi}}}^{\infty}\frac{1}{1+u^{\kappa}}du\right)}dz\\ &= \frac{1}{1+\sqrt[\kappa]{\xi}\int_{\frac{1}{\sqrt[\kappa]{\xi}}}^{\infty}\frac{1}{1+u^{\kappa}}du}\end{aligned} \tag{10}$$

where λ has totally disappeared, proving the theorem. ■

2.2 Uplink model

Referring to Figure 1b, the net interference at the typical BS is the sum of the received transmissions from all the UEs (including those inside the typical circle) except the tagged. For each UE $\mathfrak{z} \in \Psi$, we denote its distance to its serving BS by $R_{\mathfrak{z}}$.

Here, the set of interferers are the points of Ψ, which is not a PPP. To get around this difficutly, note that each point of Ψ is associated to a point in the PPP Φ of BSs, which we used above in the down link analysis. Thus, we can approximate the "spatial" average of the former to be the latter. Consequently, we can consider the locations Ψ of the interfering UEs by the locations Φ of the BSs. Specifically, for calculating the interference, we will consider that each interfering UE is placed exactly at its serving BS's location. Referring to Figure 1b, we will employ the distance $R_{\mathfrak{z}}$ between this UE and its serving BS to calculate its emitted power. We will then consider this as interference at the typical BS at distance D_z away, not $U_{\mathfrak{z}}$.

We will assume fractional power control (FPC), where each user equipment (UE) adjusts its power level in the UL direction under the control of its serving BS [Haroon et al., 2021]. FPC leads to amplifying the transmit power p at the UE based on its distance to the serving BS. If the distance is R and the FPC factor is ε, with values in $[0,1]$, then p is amplified by $R^{\varepsilon\alpha}$ to offset the path loss, which is $R^{-\alpha}$, where $\alpha > 2$ is the path loss exponent. Combining the effects of FPC, power loss and fading, the amount of power reaching the serving BS from a UE is $pGR^{-\alpha(1-\varepsilon)}$.

Referring to Figure 1b, the RV $R_{\mathfrak{z}}$ is upper bounded by $U_{\mathfrak{z}}$, otherwise the sample UE at $\mathfrak{z}$ would associate with the typical BS. Accordingly,

$$I_u = \sum_{\mathfrak{z} \in \Psi \setminus \{\mathrm{u}\}} pG_{\mathfrak{z}} R_{\mathfrak{z}}^{\alpha\varepsilon} U_{\mathfrak{z}}^{-\alpha} \tag{11}$$

In the UL, the SIR of the typical BS, at distance R from the tagged UE, is

$$\mathtt{SIR}_{\mathrm{BS}} = \frac{pGR^{-\alpha(1-\varepsilon)}}{I_u} \tag{12}$$

Consequently, the probability p_u of UL coverage is

$$p_u = \mathbb{P}[\mathtt{SIR}_{\mathrm{BS}} > \xi].$$

Referring to Figure 1b, both R and $R_{\mathfrak{z}}$ are Rayleigh distributed, i.e. $f_R(r) = f_{R_{\mathfrak{z}}}(r) = 2\lambda\pi r e^{-\lambda\pi r^2}$. Thus, $R_{\mathfrak{z}}$ ranges from 0 to R, with R ranging from an arbitrarily small positive real number to ∞. Now, the conditional UL coverage probability is defined as

$$\begin{aligned}
p_{u|R} &= \mathbb{P}[\mathtt{SIR}_{\mathrm{BS}} > \xi] \\
&= \mathbb{E}\left[\mathbb{P}\left[\frac{pGR^{-\alpha(1-\varepsilon)}}{I_u} > \xi\right]\right] \\
&= \mathbb{E}\left[\mathbb{P}\left[G > \xi p^{-1} R^{\alpha(1-\varepsilon)} I_u\right]\right] \\
&\overset{(a)}{=} \mathbb{E}\left[e^{-\xi p^{-1} I_u R^{\alpha(1-\varepsilon)}}\right] \\
&= \mathscr{L}_{I_u}(\xi p^{-1} R^{\alpha(1-\varepsilon)})
\end{aligned}$$

where $\mathscr{L}_{I_u}$ is the Laplace transform of the distribution of the I_u RV. In (a), we used the fact that $G \sim \exp(1)$, i.e. $f_G(x) = e^{-x}$, which implies that $\mathbb{P}[G > x] = e^{-x}$. Now, we decondition on R, getting

$$\begin{aligned} p_u &= \int_0^\infty \mathscr{L}_{I_u}(\xi p^{-1} R^{\alpha(1-\varepsilon)})\Big|_{R=r} f_R(r)dr \\ &= \int_0^\infty 2\widetilde{\lambda} r e^{-\widetilde{\lambda} r^2} \mathscr{L}_{I_u}(\xi p^{-1} r^{\alpha(1-\varepsilon)})dr \end{aligned} \tag{13}$$

where $\widetilde{\lambda} = \pi\lambda$. We integrate from a point just outside the origin, to skip the typical BS that resides there, to ∞ where the closest UE can possibly exist.

Next, we will embark on finding $\mathscr{L}_{I_u}$, the Laplace transform of the distribution of the RV I_u. Substituting for I_u from (11), gives

$$\begin{aligned} \mathscr{L}_{I_u}(s) &= \mathbb{E}[e^{-sI_u}] \\ &= \mathbb{E}\left[\exp\left(s\sum_{\mathfrak{z}\in\Psi} -pG_{\mathfrak{z}}R_{\mathfrak{z}}^{\alpha\varepsilon}U_{\mathfrak{z}}^{-\alpha}\right)\right] \\ &= \mathbb{E}\left[\prod_{\mathfrak{z}\in\Psi}\exp\left(-spG_{\mathfrak{z}}R_{\mathfrak{z}}^{\alpha\varepsilon}U_{\mathfrak{z}}^{-\alpha}\right)\right] \end{aligned} \tag{14}$$

In (14), for each point $\mathfrak{z} \in \Psi$ there are three RVs: $G_{\mathfrak{z}}, R_{\mathfrak{z}}, U_{\mathfrak{z}}$. The $G_{\mathfrak{z}}$ are independent of the $R_{\mathfrak{z}}$ and of the $U_{\mathfrak{z}}$. However, $U_{\mathfrak{z}}$ and $R_{\mathfrak{z}}$ are dependant in that $R_{\mathfrak{z}} < U_{\mathfrak{z}}$ (Recall that R_z is the distance between an interfering UE $\mathfrak{z}$ and its typical BS, and $U_{\mathfrak{z}}$ is the distance between the same interfering UE $\mathfrak{z}$ and the typical BS at the origin). That is $\mathbb{P}[R_{\mathfrak{z}} < x | U_{\mathfrak{z}} = x] = 1$, since if $U_{\mathfrak{z}} < R_{\mathfrak{z}}$ the interfering UE $\mathfrak{z}$ would associate with the typical BS at the origin.

Now we will resolve (14), as follows.

$$\begin{aligned} \mathscr{L}_{I_u}(s) &= \mathbb{E}_{\Psi,R_{\mathfrak{z}},G_{\mathfrak{z}}}\left[\prod_{\mathfrak{z}\in\Psi} e^{-spG_{\mathfrak{z}}R_{\mathfrak{z}}^{\alpha\varepsilon}U_{\mathfrak{z}}^{-\alpha}}\right] \\ &\overset{(a)}{=} \mathbb{E}_{\Psi,R_{\mathfrak{z}}}\left[\prod_{\mathfrak{z}\in\Psi}\mathbb{E}_{G_{\mathfrak{z}}}\left[e^{-spG_{\mathfrak{z}}R_{\mathfrak{z}}^{\alpha\varepsilon}U_{\mathfrak{z}}^{-\alpha}}\right]\right] \\ &\overset{(b)}{=} \mathbb{E}_{\Psi,R_{\mathfrak{z}}}\left[\prod_{\mathfrak{z}\in\Psi}\int_0^\infty e^{-\left(1+spR_{\mathfrak{z}}^{\alpha\varepsilon}U_{\mathfrak{z}}^{-\alpha}\right)x}dx\right] \\ &= \mathbb{E}_{\Psi,R_{\mathfrak{z}}}\left[\prod_{\mathfrak{z}\in\Psi}\frac{1}{1+spR_{\mathfrak{z}}^{\alpha\varepsilon}U_{\mathfrak{z}}^{-\alpha}}\right] \end{aligned} \tag{15}$$

In (a) we used the fact that the $G_{\mathfrak{z}}$ are iid and in (b) we used the fact that $f_{G_{\mathfrak{z}}}(x) = e^{-x}$.

Next, we consider the expectation with respect to Ψ, to uncondition on $U_{\mathfrak{z}}$, the distance between every point $\mathfrak{z} \in \Psi$ and the origin. We will use for this expectation a PGFL, since $U_{\mathfrak{z}}$ is distributed differently for each point $\mathfrak{z} \in \Psi$.

Referring to Figure 1b, and based on our approximation, each point $\mathfrak{z} \in \Psi$ will be relocated to the position of the associated point $z \in \Phi$. That is, we will consider

each interfering UE at point $z \in \Phi$ emitting power $pR_{\mathfrak{z}}^{\alpha\varepsilon}$, but causing interference with this same power at the typical BS, at a distance D_z based on the UE relocation. This allows us to write

$$\mathbb{E}_{\Psi}\left[\prod_{\mathfrak{z}\in\Psi} f(\mathfrak{z})\right] \approx \mathbb{E}_{\Phi}\left[\prod_{z\in\Phi} f(z)\right] = e^{-\lambda\int_{\mathbb{R}^2}(1-f(x))}.$$

Substituting for $f(y)$ from (15), converting to polar coordinates, and substituting for the angle integral by 2π, then

$$\begin{aligned}\mathscr{L}_{I_u}(s) &= \mathbb{E}_{R_{\mathfrak{z}}}\left[\mathbb{E}_{\Phi}\left[\prod_{z\in\Phi}\frac{1}{1+spR_{\mathfrak{z}}^{\alpha\varepsilon}D_z^{-\alpha}}\right]\right] \\ &= \mathbb{E}_{R_{\mathfrak{z}}}\left[e^{-2\pi\lambda\int_0^{\infty}\frac{1}{1+(sp)^{-1}R_{\mathfrak{z}}^{-\alpha\varepsilon}x^{\alpha}}xdx}\right] \end{aligned} \tag{16}$$

The distance $R_{\mathfrak{z}}$ is lower bounded by $U_{\mathfrak{z}}$, for if $R_{\mathfrak{z}} < U_{\mathfrak{z}}$, the UE at $\mathfrak{z}$ would associate with the typical BS. But note that $U_{\mathfrak{z}}$ has been replaced now, through PP relocation, by $D_{\mathfrak{z}}$.

We will now apply the last expectation, $\mathbb{E}_{R_{\mathfrak{z}}}$, noting that the distribution of $R_{\mathfrak{z}}$ is Rayleigh. In light of (16), using the Rayleigh distribution $f_{R_{\mathfrak{z}}}(y) = 2\lambda\pi y e^{-\lambda\pi y^2}$, we have

$$\begin{aligned}\mathscr{L}_{I_u}(s) &= e^{-2\pi\lambda\int_0^{\infty}\left(\mathbb{E}_{R_{\mathfrak{z}}}\left[\frac{1}{1+(sp)^{-1}R_{\mathfrak{z}}^{-\alpha\varepsilon}x^{\alpha}}\right]\right)xdx} \\ &= e^{-2\pi^2\lambda^2\int_0^{\infty}x\int_0^{x^2}\frac{e^{-\lambda\pi u}}{1+(sp)^{-1}u^{-\alpha\varepsilon/2}x^{\alpha}}dudx} \end{aligned} \tag{17}$$

where $u = y^2$. Recall that $D_z^{-\alpha}$ and $R_{\mathfrak{z}}$ are dependent in that if $D_z = x$ then $R_{\mathfrak{z}} < x$. From (11) and (13), it follows that

$$\begin{aligned}\mathscr{L}_{I_u}(\xi p^{-1}r^{\alpha(1-\varepsilon)}) &= e^{-2\pi^2\lambda^2\int_0^{\infty}x\int_0^{x^2}\frac{e^{-\lambda\pi u}}{1+(sp)^{-1}u^{-\alpha\varepsilon/2}x^{\alpha}}dudx} \\ &= e^{-2\pi^2\lambda^2\int_0^{\infty}x\int_0^{x^2}\frac{\xi r^{\alpha(1-\varepsilon)}e^{-\lambda\pi u}}{\xi r^{\alpha(1-\varepsilon)}+u^{-\alpha\varepsilon/2}x^{\alpha}}dudx} \end{aligned} \tag{18}$$

From (13) and (18), we get

$$p_u = 2\widetilde{\lambda}\int_0^{\infty} re^{-\widetilde{\lambda}r^2}e^{-2\widetilde{\lambda}^2\xi r^{2\kappa(1-\varepsilon)}\int_0^{\infty}x\int_0^{x^2}\frac{e^{-\widetilde{\lambda}u}}{\xi r^{2\kappa(1-\varepsilon)}+u^{-\varepsilon\kappa}x^{2\kappa}}dudx}dr \tag{19}$$

where $\widetilde{\lambda} = \pi\lambda$ and $\kappa = \alpha/2$.

From (19), it *appears* that the UL coverage probability p_u is dependent on the BS density λ. However, we will show in Theorem 2 below that the presence of λ in (19) is superfluous.

Theorem 2: Under the stochastic geometric model of the cellular UL system, the UL coverage probability p_u is independent of the BS density λ.

Proof: The proof is attained through a sequence of changes of variables. Starting with (19), use the substitution $v = r^2$ to get

$$p_u = \widetilde{\lambda} \int_0^{\infty} e^{-\widetilde{\lambda} v} e^{-2\widetilde{\lambda}^2 \xi v^{\kappa(1-\varepsilon)} \int_0^{\infty} x \int_0^{x^2} \frac{e^{-\widetilde{\lambda} u}}{\xi v^{\kappa(1-\varepsilon)} + u^{-\varepsilon\kappa} x^{2\kappa}} du dx} dv$$

Use $y = x^2$ to get

$$p_u = \widetilde{\lambda} \int_0^{\infty} e^{-\widetilde{\lambda} v} e^{-\widetilde{\lambda}^2 \xi v^{\kappa(1-\varepsilon)} \int_0^{\infty} \int_0^{y} \frac{e^{-\widetilde{\lambda} u}}{\xi v^{\kappa(1-\varepsilon)} + u^{-\varepsilon\kappa} y^{\kappa}} du dy} dv$$

Use $x = \widetilde{\lambda} u$ to get

$$p_u = \widetilde{\lambda} \int_0^{\infty} e^{-\widetilde{\lambda} v} e^{-\widetilde{\lambda} \xi v^{\kappa(1-\varepsilon)} \int_0^{\infty} \int_0^{\widetilde{\lambda} y} \frac{e^{-x}}{\xi v^{\kappa(1-\varepsilon)} + \left(\frac{x}{\widetilde{\lambda}}\right)^{-\varepsilon\kappa} y^{\kappa}} dx dy} dv$$

Use $z = \widetilde{\lambda} v$ to get

$$p_u = \int_0^{\infty} e^{-z} e^{-\widetilde{\lambda} \xi z^{\kappa(1-\varepsilon)} \int_0^{\infty} \int_0^{\widetilde{\lambda} y} \frac{e^{-x}}{\xi z^{\kappa(1-\varepsilon)} + x^{-\varepsilon\kappa} \left(\widetilde{\lambda} y\right)^{\kappa}} dx dy} dz$$

Finally, use $u = \widetilde{\lambda} y$ to get

$$p_u = \int_0^{\infty} e^{-z\left(1 + \xi z^{\kappa(1-\varepsilon)-1} \int_0^{\infty} \int_0^{u} \frac{e^{-x}}{\xi z^{\kappa(1-\varepsilon)} + x^{-\varepsilon\kappa} u^{\kappa}} dx du\right)} dz \tag{20}$$

where λ has totally disappeared, proving the theorem. ■

3 Conclusions

In this article we have proven two theorems that go against established belief in the SG cellular modelling literature. Namely, we have proved that under the stochastic geometric model, the coverage probability in either DL and UL is independent of the BS density. This finding calls for a revisit to a large body of published results.

References

Ali et al., 2019. Ali, S., Aslam, M., and Ahmed, I. (2019). Uplink coverage probability and spectral efficiency for downlink uplink decoupled dense heterogeneous cellular network using multi-slope path loss model. *Telecommunication systems*, 72(4):505–516 1.

Andrews et al., 2011. Andrews, J., Baccelli, F., and Ganti, R. (2011). A tractable approach to coverage and rate in cellular networks. *IEEE Transactions on Communicationsy*, 59(11):3122–3134.

Andrews et al., 2016. Andrews, J., Gupta, A., and Dhillon, H. (2016). A primer on cellular network analysis using stochastic geometry. *ArXiv*.

Bai and Heath, 2015. Bai, T. and Heath, R. (2015). Coverage and rate analysis for millimeter-wave cellular networks. *IEEE Transactions on Wireless Communications*, 14(2):1100–1114.

Blaszczyszyn et al., 2018. Blaszczyszyn, B., Haenggi, M., Keeler, P., and Mukherjee, S. (2018). *Stochastic Geometry Analysis of Cellular Networks*. Cambridge University Press, Cambridge.

Chen and Yuan, 2019. Chen, J. and Yuan, C. (2019). Coverage probability and average rate of downlink user-centric wireless cellular networks with composite κ-μ shadowed and lognormal shadowed fading. *IET Communication*, 13(17):2805–2813.

ElSawy et al., 2017. ElSawy, H., Sultan, A., Alouini, M., and Win, M. (2017). Modeling and analysis of cellular networks using stochastic geometry: A tutorial. *IEEE Communications Surveys and Tutorials*, 19(1):167–203.

Fadouol, 2020. Fadouol, M. (2020). Rate and coverage analysis in multi-tier heterogeneous network using stochastic geometry approach. *Ad Hoc Network*, 98.

Gao et al., 2019. Gao, Y., Yang, S., Wu, S., Wang, M., and Song, X. (2019). Coverage probability analysis for mmwave communication network with absf-based interference management by stochastic geometry. *IEEE Access*, 7:133572–133582.

Haenggi, 2012. Haenggi, M. (2012). *Stochastic Geometry for Wireless Networks*. Cambridge University Press, Cambridge.

Haroon et al., 2021. Haroon, M., Muhammad, F., Abbas, Z., Abbas, G., Ahmed, N., and Kim, S. (2021). Proactive uplink interference management for nonuniform heterogeneous cellular networks. *IEEE Access*, 8:55501–555123.

Herath et al., 2018. Herath, P., Tellambura, C., and Krzymień, W. (2018). Coverage probability analysis of three uplink power control schemes: Stochastic geometry approach. *EURASIP journal on wireless communications and networking*, 1:1–14.

Jia et al., 2019. Jia, X., Fan, Q., Xu, W., and Yang, L. (2019). Cross-tier dual-connectivity designs of three-tier hetnets with decoupled uplink/downlink and global coverage performance evaluation. *IEEE Access*, 7:16816–168361.

Kouzayha et al., 2018. Kouzayha, N., Dawy, Z., Andrews, J., and ElSawy, H. (2018). Joint downlink/uplink rf wake-up solution for iot over cellular networks. *IEEE Transactions on Wireless Communications*, 17(3):1574–1588.

Kouzayha et al., 2021. Kouzayha, N., Elsawy, H., Dahrouj, H., and Al-Naffouri, T. (2021). Meta distribution of downlink sir for binomial point processes. *IEEE Wireless Communications Letters*, 10(7):1557–1561.

Kundu et al., 2020. Kundu, A., Pal, R., Kumar, M., and Sreejith, T. (2020). Uplink and downlink performance bounds for full duplex cellular networks. In *2020 IEEE International Black Sea Conference on Communications and Networking (BlackSeaCom)*, Odessa, Ukrain.

Lee et al., 2013. Lee, C., Shih, C., and Chen, Y. (2013). Stochastic geometry based models for modeling cellular networks in urban areas, wireless networks. *Wireless networks*, 19(6):1063–1072.

Lei et al., 2018. Lei, J., Chen, H., and Zhao, F. (2018). Stochastic geometry analysis of downlink spectral and energy efficiency in ultradense heterogeneous cellular networks. *Mobile Information Systems*, 2018.

Liu et al., 2020a. Liu, ., Baudais, J., and Mary, P. (2020a). A tractable coverage analysis in dynamic downlink cellular networks. In *2020 IEEE 21st International Workshop on Signal Processing Advances in Wireless Communications (SPAWC)*, pages 1–5. IEEE.

Liu et al., 2020b. Liu, C., Shen, Y., and Lee, C. (2020b). Energy-efficient activation and uplink transmission for cellular iot. *IEEE Internet of Things Journal*, 7(2):906–921.

Liu and Zhang, 2020. Liu, Q. and Zhang, Z. (2020). The analysis of coverage probability,ase and ee in heterogeneous ultra-dense networks with power control. *Digital Communications and Networks*, 6(4):524–533.

Mariam et al., 2021. Mariam, H., Ahmed, I., and Aslam, M. (2021). Coverage probability of uplink millimeter wave cellular network with non-homogeneous interferers' point process. *Physical Communication*, 45.

Okegbile et al., 2021. Okegbile, S., Maharaj, B., and Alfa, A. (2021). Stochastic geometry approach towards interference management and control in cognitive radio network: A survey. *Computer Communications*, 166(15):174–195.

Ouamri et al., 2020. Ouamri, M., Oteşteanu, M., Isar, A., and Azni, M. (2020). Coverage, handoff and cost optimization for 5g heterogeneous network. *Physical Communication*, 39(5).

Sadeghabadi et al., 2020. Sadeghabadi, E., Abarghouyi, S., Makki, B., Kenari, M., and Svensson, T. (2020). Asynchronous downlink massive mimo networks: A stochastic geometry approach. *IEEE Transactions on Wireless Communications*, 19(1):579–594.

Tang et al., 2020. Tang, X., Xu, X., and Haenggi, M. (2020). Meta distribution of the sir in moving networks. *IEEE Transactions on Communication*, 68(6):3614–3626.

Wang and Gursoy, 2019. Wang, X. and Gursoy, M. (2019). Coverage analysis for energy-harvesting uav-assisted mmwave cellular networks. *IEEE Journal on Selected Areas in Communications*, 37(12):2832–2850.